Supplementary Materials

Nature Biotechnology: doi:10.1038/nbt.2884

Fig. S1

a

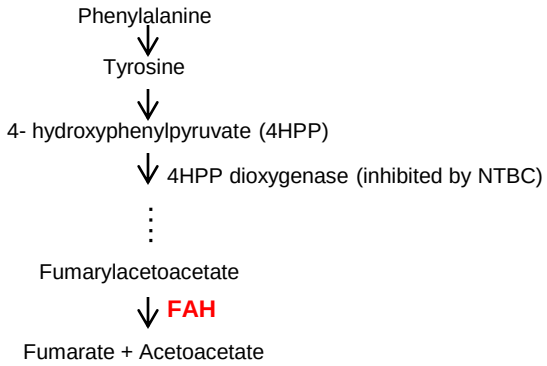

b

GTTGAACTTTGAAAATATTTTCCCTTTGCTCTGTAAGCCACAGTGACCCAGAGCATCGGG
TCATCTAGATTCTTACCAACTTTCTCCATGGCAGGCTTTCTTCGTAGGCCCTGGGAACAG
ATTCGGAGAGCCAATCCCCATTTCCAAAGCCCATGAACACATTTTCGGGATGGTCCTCAT
GAACGACTGGAGCAGTAATGCCTGGTGGCCCAGCTTCCTCTGATGTTCTGTTCTTAGGGG
CACACACAGGAGTTGGGTATGGGACAGGAGGCCTAAGTACTACAGGGGTGATACCATGCA
GACTTCTGACTCTGTGGGTGTGGGGCAGTCACAGCTTCCCTGAGTAGCTTTCTCATAAGT
GGAAGGATGGAGCTGACAGAACCTAAAGCTTTATCAAGCCCTACACACTCCACTCACTGT

Wild type = G/G Fah splicing mutant = A/A

c

Fah seq CCTCATGAACGACTGGAGCAGTAATGCCTGGTGG

FAH 1
ACTGGAGCAGTAATGCCTGGTGG
Fah1a CACCGACTGGAGCAGTAATGCCTGG
Fah1b AAACCCAGGCATTACTGCTCCAGTC

FAH 2
ACGACTGGAGCAGTAATGCCTGG
Fah2a CACCGACGACTGGAGCAGTAATGCC
Fah2b AAACGGCATTACTGCTCCAGTCGTC

FAH 3
CCTCATGAACGACTGGAGCAGTA
Fah3a CACCGTACTGCTCCAGTCGTTCATG
Fah3b AAACCATGAACGACTGGAGCAGTAC

d

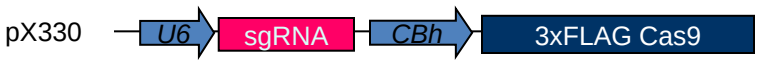

Supplementary Figure 1. The Fah$^{mut/mut}$ mouse model of hereditary tyrosinemia type I (HTI). (a) FAH is the last enzyme in the tyrosine metabolic pathway. FAH deficiency causes accumulation of toxic metabolites, such as fumarylacetoacetate (FAA). NTBC blocks upstream pathway and rescues liver damage. (b) Genomic sequence of Fah$^{mut/mut}$ mice. The G->A splicing mutation is marked in green. Exon8 is underlined. (c) Sequences of Fah sgRNA (PAM in orange) and oligos for cloning sgRNA (BbsI sites in red). (d) The pX330 plasmid co-expresses sgRNA and Cas9 (adapted from Hsu, et al, 2013).

Fig. S2

a

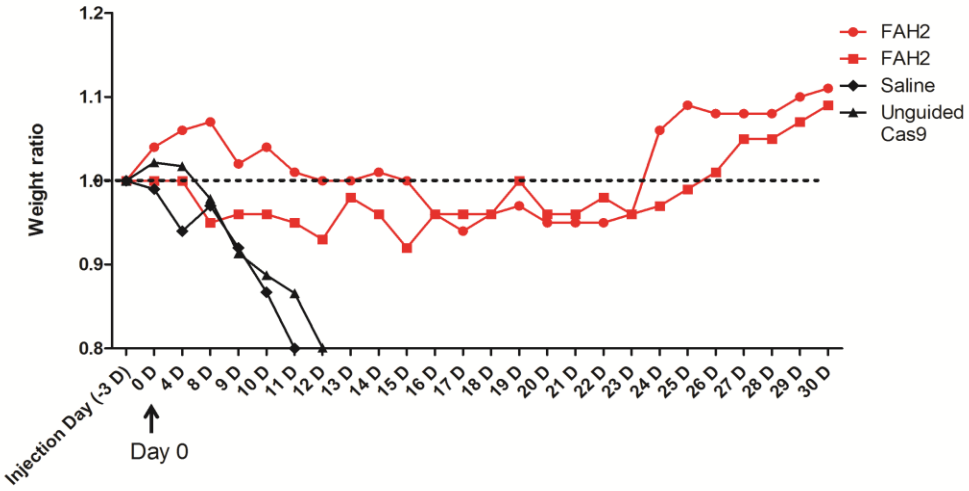

b

	Reach euthanasia criteria	Not reach euthanasia criteria
Controls	5	0
FAH Treated	0	5

c

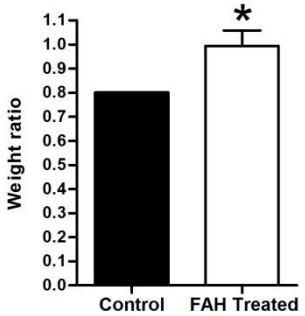

Supplementary Figure 2. Hydrodynamic injection of CRISPR in the liver rescues weight loss in Fah deficient mice. (a) *Fah*$^{mut/mut}$ mice were injected with saline only, ssDNA oligo plus pX330 (unguided Cas9), or ssDNA oligo plus pX330 expressing Fah sgRNA 2 (FAH2). Body weight was monitored over time and normalized to pre-injection. Arrow indicates withdrawal of NTBC water (defined as Day 0, which is 3 days post injection). (b) Summary of conditions of experimental mice in first round of NTBC withdrawal in Fig. 1 and Fig. S2a. Fisher's exact test was performed. $P<0.01$. (c) Weight of experimental mice at endpoints in first round of NTBC withdrawal (Day 30) in Fig. 1 and Fig. S2a. $P<0.01$ (N=5), using an unpaired t-test.

Nature Biotechnology: doi:10.1038/nbt.2884

Fig. S3

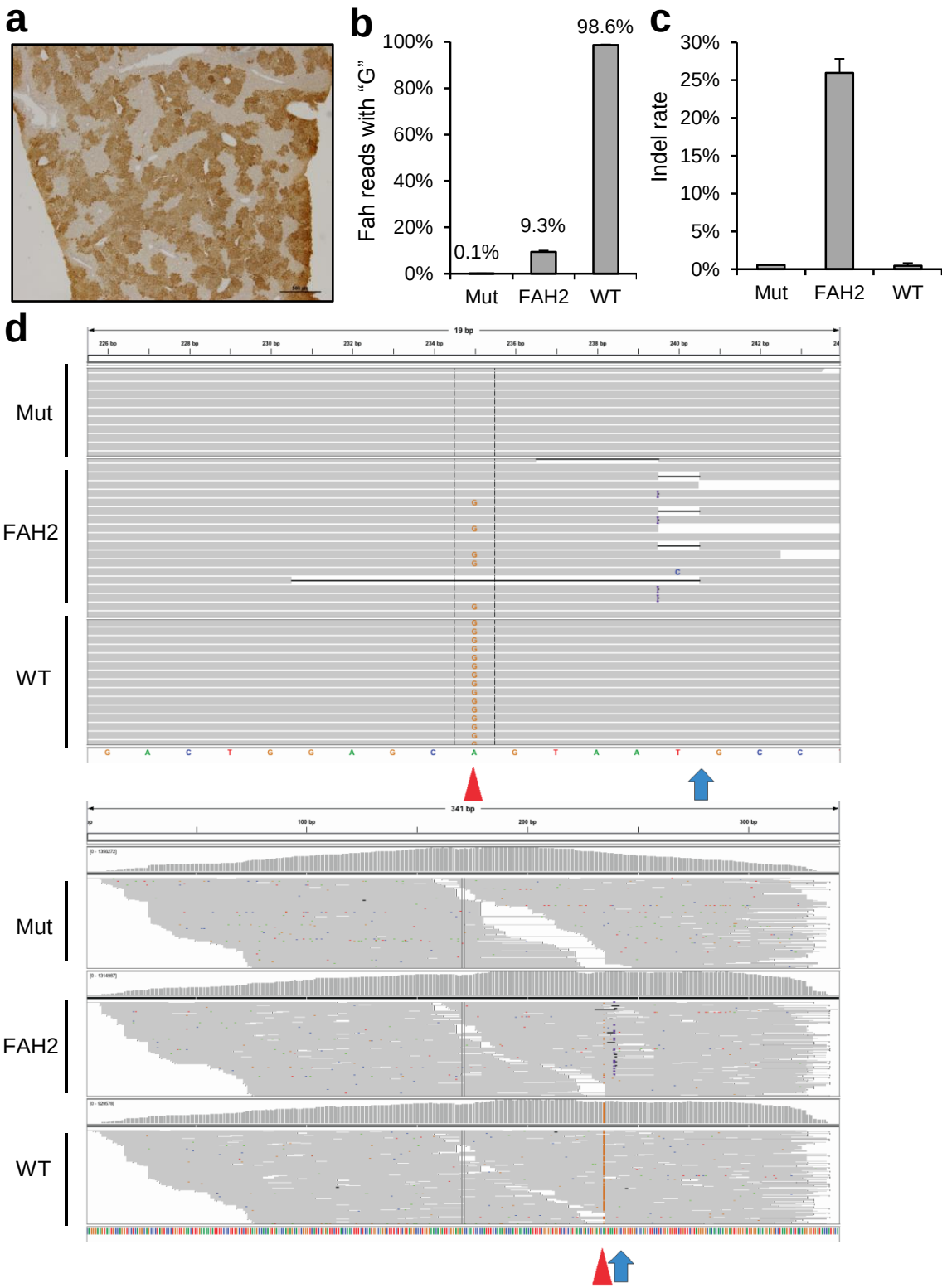

Supplementary Figure 3. CRISPR generates Fah^{+} hepatocytes in the liver. (a) Low magnification microscopic images of Fah IHC staining in *Fah$^{mut/mut}$* mice treated with FAH2 at 30 days off NTBC water. 33.5% ± 3.3% hepatocytes stained Fah^{+}. Control samples showed 0.01±0.02% Fah^{+} (image not shown here). P<0.01 (N=3). **(b)** Fah repair rate at genomic level determined by next-generation sequencing reads with "G". Fah genomic region was sequenced in total liver genomic DNA from wildtype mice (WT) and *Fah$^{mut/mut}$* mice injected with unguided Cas9 (Mut) or FAH2 (FAH2). Error bars are s.d. (N=2). **(c)** Percentage of Fah indels. **(d)** Representative sequencing reads. Upper panel: 19bp region flanking the Fah mutation. Lower panel: Fah PCR region. Thick black bars represent deletions and purple "I" represent insertions. Red arrowheads indicate Fah G->A mutation site. Blue arrows denote Cas9 cutting sites. "G" in the wildtype Fah alleles is marked in yellow.

Nature Biotechnology: doi:10.1038/nbt.2884

Fig. S4

a

ID	Sequence (20nt+PAM)	score	mismatches	UCSC gene	locus
	ACTGGAGCGGTAATGCCTGGTGG	61.1	1MMs [9]	Fah	chr7:-91743949
1	GCTGCAGCAGTAATGCCTGCCAG	1.5	3MMs [1:5:20]		chr5:-27804984
2	ACTGAAGGAGAAATGCCTGGAAG	1.4	3MMs [5:8:11]	NM_026599	chr9:-71498065
3	ACTGAAGCAGTAAAGCCTGGTGG	1.2	2MMs [5:14]		chr12:-25915865
4	TCTGAAGCAGTAGTGCCTGGGGG	1.2	3MMs [1:5:13]		chr4:-76460945
5	AATGTATTAGTAATGCCTGGCAG	0.9	4MMs [2:5:7:8]		chr15:-50350732
6	ACTGGTGATGTAATGCCTGGGGG	0.9	3MMs [6:8:9]		chr10:-85954983
7	GCTGGTGCAGTGATGCCTGGAGG	0.9	3MMs [1:6:12]	NM_001174074	chr18:+25659816
8	TGTGCAGCAGAAATGCCTGGGAG	0.8	4MMs [1:2:5:11]		chr16:-17033219
9	CCAGATGCAGTAATGCCTGGGAG	0.8	4MMs [1:3:5:6]		chr6:-121892833
10	CGGGGTGCAGTAATGCCTGGCAG	0.8	4MMs [1:2:3:6]		chr7:-131053232
11	ATTAGAGGAGAAATGCCTGGTGG	0.8	4MMs [2:4:8:11]		chr14:-60579615
12	GCTATAGCAGTGATGCCTGGCAG	0.7	4MMs [1:4:5:12]		chr14:+11448305
13	ACTAGAGCACTAATACCTGGAAG	0.7	3MMs [4:10:15]		chr16:+67529873
14	AGTGAAGTAGTAATGCCTGAGAG	0.7	4MMs [2:5:8:20]	NM_018852	chr2:+66325479
15	TCTTTAGCAGTATTGCCTGGCAG	0.6	4MMs [1:4:5:13]		chr7:+36322925
16	CCACGAGCAGTACTGCCTGGCAG	0.6	4MMs [1:3:4:13]		chr5:+111609584
17	TCAAGAGCAGTACTGCCTGGAGG	0.6	4MMs [1:3:4:13]		chr1:+4859691
18	GCTTGAGCATTAATGCATGGCAG	0.6	4MMs [1:4:10:17]		chr7:+151944808
19	ACAGGAAGGGTAATGCCTGGAAG	0.6	4MMs [3:7:8:9]		chr11:-25262208
20	AAGGGACCAGCAATGCCTGGCAG	0.5	4MMs [2:3:7:11]		chr3:-152548541

b

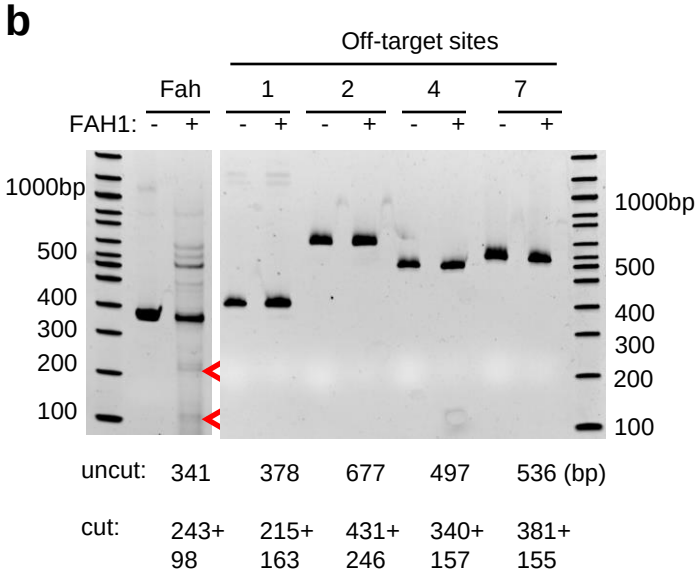

Supplementary Figure 4. Assessing off-target cutting of FAH1. (a) Top 20 potential off-target sites for FAH1 in the mouse genome. Score is likelihood of off-target binding. The one nucleotide mismatch with wildtype Fah is highlighted in red. (b) Surveyor assay in mouse 3T3 cells transfected with unguided Cas9 (-) or FAH1 (+). Predicted size of uncut and cut bands are indicated. Arrowheads denote surveyor nuclease cleaved fragments of the Fah PCR products.

Fig. S5

a

ID	sequence	score	mismatches	UCSC gene	locus
	ACGACTGGAGCGGTAATGCCTGG	49.2	1MMs [12]	Fah	chr7:-91743952
1	ACAACTGGAGCAGAAATGCCAGG	1.4	2MMs [3:14]		chr2:-27426420
2	GGGACTCCAGCAGTAATGCCCAG	0.9	4MMs [1:2:7:8]		chr9:-23503647
3	TCCATTGGGGCAGTAATGCCAGG	0.8	4MMs [1:3:5:9]		chr3:+51805010
4	ACGAATGTATTAGTAATGCCTGG	0.7	4MMs [5:8:10:11]		chr15:-50350735
5	ATGTCTGCAGCAGTAATGCAAGG	0.7	4MMs [2:4:8:20]		chr10:+28923493
6	AGCACTGAAGCAGTAAAGCCTGG	0.6	4MMs [2:3:8:17]		chr12:-25915868
7	ATTACTGGAACAATAATGCCCAG	0.5	4MMs [2:3:10:13]		chr4:+73190436
8	AGGATTGGAACAGTAATGACTGG	0.5	4MMs [2:5:10:19]	NM_172546	chr10:-3212116
9	ACCACAGGCACAGTAATGCCTAG	0.5	4MMs [3:6:9:10]		chr16:-69906257
10	ACAAGAGGAGCAGTAATGCAGGG	0.4	4MMs [3:5:6:20]		chr14:-65240909
11	ATAAGTGGAGCAGTTATGCCAAG	0.4	4MMs [2:3:5:15]		chr7:-101738529
12	ATGATTAGAGCATTAATGCCTGG	0.4	4MMs [2:5:7:13]		chr7:+15076636
13	ACGATTAGAACAGTAACGCCTGG	0.4	4MMs [5:7:10:17]		chr6:+83118712
14	ACAACTAAAGCAGTAATGACCAG	0.3	4MMs [3:7:8:19]		chr18:+81123732
15	AGGACTGAAGAAATAATGCCCAG	0.3	4MMs [2:8:11:13]		chr14:+103601624
16	AGAGCTGGAGCAGTAATACCTAG	0.3	4MMs [2:3:4:18]		chr5:-30273905
17	AATATTGGAGCAGTAATTCCTAG	0.3	4MMs [2:3:5:18]		chr14:-102078839
18	ATGACTGGAGCAGTTATGTCGGG	0.3	3MMs [2:15:19]		chr1:-122355339
19	AGGACTAGTGCAGTAATGCAAAG	0.3	4MMs [2:7:9:20]		chr12:-112339333
20	GAGCCTGGAGCAGTACTGCCTGG	0.3	4MMs [1:2:4:16]		chr14:-60518309

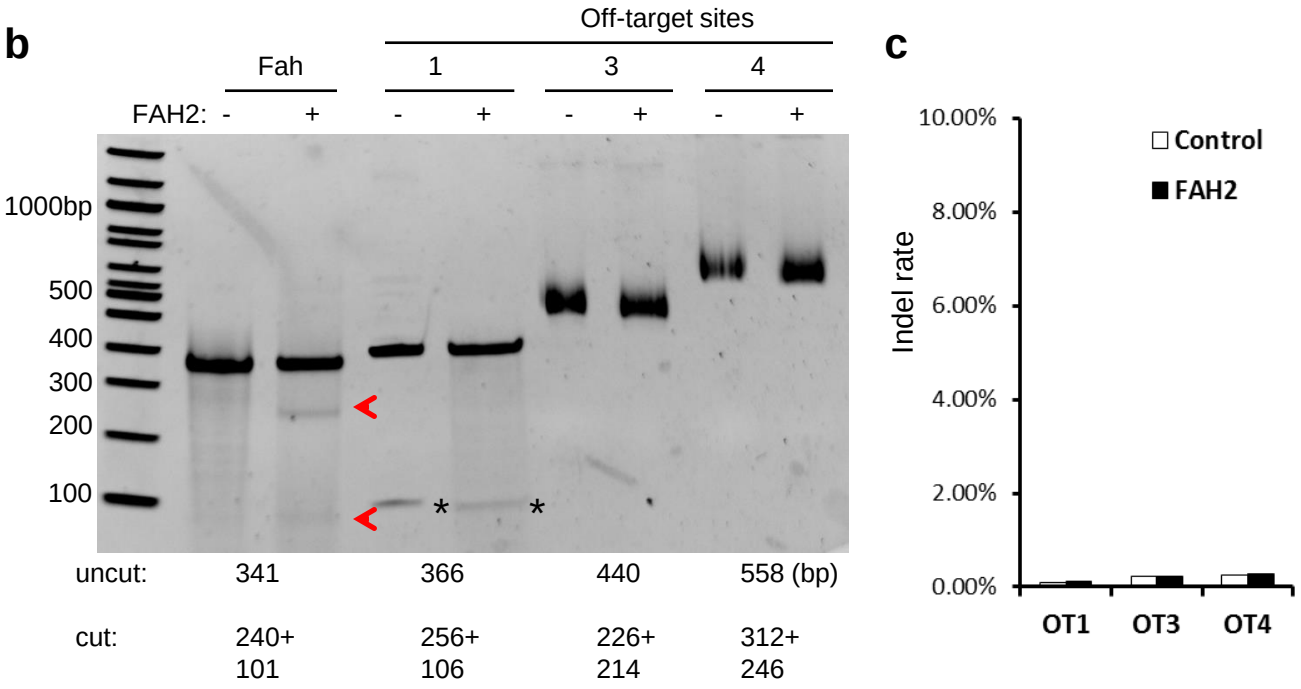

Supplementary Figure 5. Assessing off-target cutting of FAH2. (a) Top 20 potential off-target sites for FAH2 in the mouse genome. Score is likelihood of off-target binding. The one nucleotide mismatch with wildtype Fah is highlighted in red. (b) Surveyor assay in mouse 3T3 cells transfected with unguided Cas9 (-) or FAH2 (+). Predicted size of uncut and cut bands are indicated. Red arrowheads denote surveyor nuclease cleaved fragments of the Fah PCR products. Asterisks denote non-specific bands. (c) The percentage of indels at off-target sites of FAH2 determined by next-generation sequencing. OT1, OT3, OT4 indicate Fah off-target sites 1, 3, 4.

Fig. S6

a

ID	sequence	score	mismatches	UCSC gene	locus
	TACCGCTCCAGTCGTTCATGAGG	100	1MMs [4]	Fah	chr7:+91743963
1	AATTGCTTCAGTCGTTCATGAAG	2.6	3MMs [1:3:8]		chr18:+24014164
2	TTCAGCTCCAGTAGTTCATGTGG	1.1	3MMs [2:4:13]		chr13:+48556695
3	TGCTTCTGCATTCGTTCATGCAG	0.8	4MMs [2:5:8:11]		chr11:+100913652
4	TGGTTCTCCAGGCGTTCATGGGG	0.7	4MMs [2:3:5:12]		chr2:+74892464
5	CACTGCATGAGTCGTTCATGAGG	0.6	4MMs [1:7:8:9]		chr8:+36555755
6	TCTTACTCCAGTTGTTCATGGAG	0.6	4MMs [2:3:5:13]		chrX:+89772175
7	TCCTCCACCATTCGTTCATGAAG	0.5	4MMs [2:5:7:11]		chr19:-26357942
8	AACTGCTGCTGTTGTTCATGGAG	0.5	4MMs [1:8:10:13]		chr11:+104770974
9	TACTCCTCCAGTAGTTCATCTAG	0.5	3MMs [5:13:20]		chr10:-23843629
10	TAGTCCTGCAGTCGGTCATGTGG	0.4	4MMs [3:5:8:15]		chr14:-99272709
11	TGCTGCTCCCTACGTTCATGAAG	0.4	4MMs [2:10:11:12]		chr15:+12543054
12	TGCTGCTCCTTCCGTTCATGAGG	0.4	4MMs [2:10:11:12]		chr1:+57569091
13	TTGTGTTCCAGTCGTTTATGGGG	0.4	4MMs [2:3:6:17]		chr8:-108055143
14	TACTGCTCCTGTGGTTTATGGAG	0.4	3MMs [10:13:17]		chr13:+81182469
15	GCCTGCTCCAGCCGTTCATCCGG	0.3	4MMs [1:2:12:20]		chr8:-110111644
16	TAATGGTGCAGTTGTTCATGAAG	0.3	4MMs [3:6:8:13]		chr4:+9246640
17	TTCTGCTCCAGTTGATCATGGAG	0.3	3MMs [2:13:15]		chr1:-135239152
18	TACTCCTGCAGGAGTTCATGTGG	0.3	4MMs [5:8:12:13]	NM_001033260	chr10:-62126645
19	TACTGCTTCCATAGTTCATGGGG	0.3	4MMs [8:10:11:13]		chr10:-118436555
20	TACTGGTGAAGCCGTTCATGAAG	0.2	4MMs [6:8:9:12]		chr13:+24639232

b

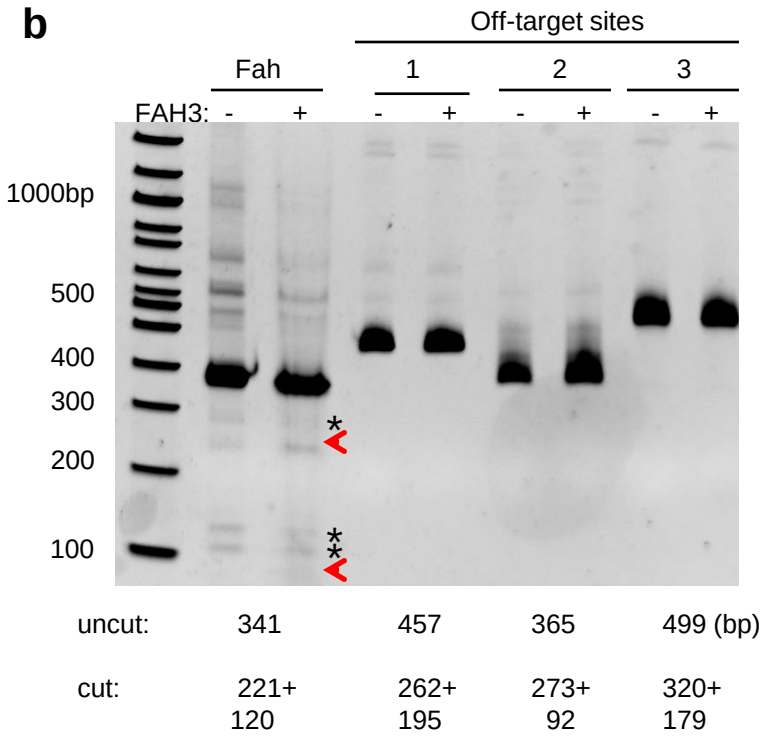

uncut:	341	457	365	499 (bp)
cut:	221+ 120	262+ 195	273+ 92	320+ 179

Supplementary Figure 6. Assessing off-target cutting of FAH3. (a) Top 20 potential off-target sites for FAH3 in the mouse genome. Score is likelihood of off-target binding. The one nucleotide mismatch with wildtype Fah is highlighted in red. (b) Surveyor assay in mouse 3T3 cells transfected with unguided Cas9 (-) or FAH3 (+). Predicted size of uncut and cut bands are indicated. Arrowheads denote surveyor nuclease cleaved fragments of the Fah PCR products. Asterisks indicate non-specific bands.

Nature Biotechnology: doi:10.1038/nbt.2884

Fig. S7

a

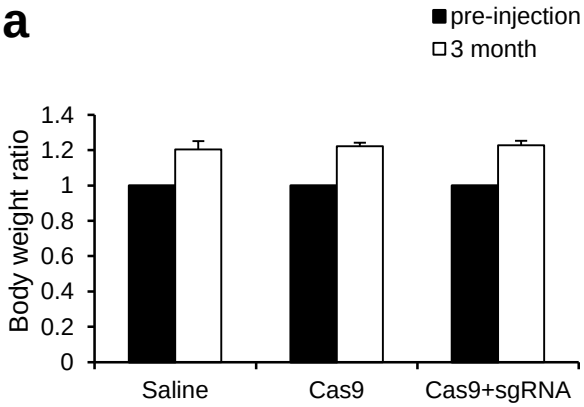

b

	Mice examined	Mice with liver hyperplasia or tumor
Saline	5	0
Cas9	5	0
Cas9+sgRNA	5	0

Supplementary Figure 7. Hydrodynamic injection of CRISPR is safe in mice. (a) Body weight of FVB mice injected with saline or Cas9 plasmids. Eight weeks old FVB mice were injected with indicated plasmids. Error bars are s.d. (N=5). (b) Numbers of mice showing liver hyperplasia or tumor at 3 month post injection.

Nature Biotechnology: doi:10.1038/nbt.2884

Fig. S8

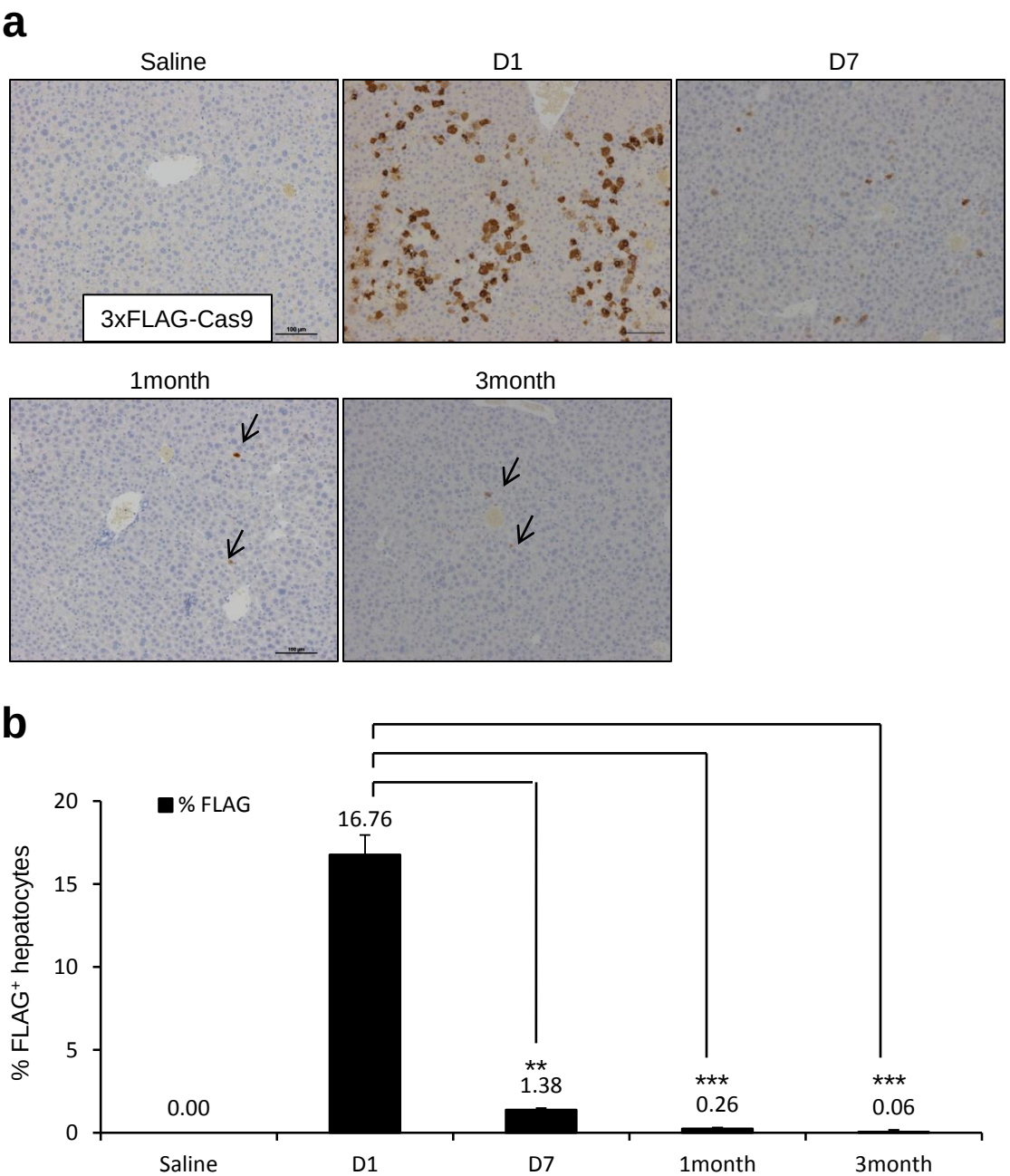

Supplementary Figure 8. Evaluating pX330 plasmid expression in the liver. (a) FVB mice were hydrodynamically injected with 60μg pX330 plasmid. Livers were harvested at indicated time points and stained with a FLAG tag specific antibody which detects 3xFLAG tagged Cas9 protein. Representative IHC images are shown. Arrows denote FLAG positive cells. Scale bar=100μm. (b) Quantification of FLAG$^+$ cells. Numbers are mean ± s.d.. **, p<0.001. ***, p<0.0001. (N=3) using one-way ANOVA.

Nature Biotechnology: doi:10.1038/nbt.2884

Supplementary Table 1. Primer sequences.

ID	Sequence (5'->3')	Notes
Fah.F5	TTCTACTCTTCTCGGCAGCA	RT-PCR primer with Fah.R9
Fah.F8	AGAGCCAATCCCCATTTCCA	QPCR primer with Fah.R9
Fah.R9	CGGGGAGATTGTGGTTCCAA	
FAH_PointM_F	CAGGGAAGTAATGCCAGGTC	Fah PCR primers
FAH_PointM_R	TGCATGGTATCACCCCTGTA	
FAH1-OT1F	CCTTCACAGAGCGGGTTTTC	FAH1 Off target site 1
FAH1-OT1R	AGTGAAGCCCTGTAGCCATT	
FAH1-OT2F	TAACTCTGGCAACCCCTCTG	FAH1 Off target site 2
FAH1-OT2R	TTTCGCTTGTGTGTCAGTGG	
FAH1-OT4F	CTGGAGTCTCACAACAGGGA	FAH1 Off target site 4
FAH1-OT4R	GACTACTCCTAGGCCTGCAG	
FAH1-OT7F	TCCTGACTTGGCTAGAGTGC	FAH1 Off target site 7
FAH1-OT7R	GCTCAGGGAAGGAAGGACTT	
FAH2-OT1F	ACTCACACTGTCATCCCTCG	FAH2 Off target site 1
FAH2-OT1R	GTTCCCACTACCACAATGCC	
FAH2-OT3F	TCTGGGGATTGGGTAGTGAC	FAH2 Off target site 3
FAH2-OT3R	GTCCTGGCCCGGATTATACA	
FAH2-OT4F	AAGGCATTGGAAGGGCTAAT	FAH2 Off target site 4
FAH2-OT4R	GCTAAACACTTGGGGCATGT	
FAH3-OT1F	TCCCAGCCAACAAGATGCTA	FAH3 Off target site 1
FAH3-OT1R	TGCAGCTGTGATAGGAACCA	
FAH3-OT2F	CATTCCATCGCTTCGGTCTG	FAH3 Off target site 2
FAH3-OT2R	ACATCTCGTCTTCAGTGGCA	
FAH3-OT3F	AACAGTGTCTCCTGTAGCCC	FAH3 Off target site 3
FAH3-OT3R	CGCCATTTCCAGTGAGCTAC	

Supplementary Table 2. Oligo sequences. The G nucleotide to correct the A->G mutation is underlined.

ID	Sequence (5'->3')

Fah ssDNA	GCTTTCTTCGTAGGCCCTGGGAACAGATTCGGAGAGCCAATCCCCATTTCCAAAGC CCATGAACACATTTTCGGGATGGTCCTCATGAACGACTGGAGCGGTAATGCCTGGT GGCCCAGCTTCCTCTGATGTTCTGTTCTTAGGGGCACACACAGGAGTTGGGTATGG GACAGGAGGCCTAAGTACTACAGGGGTGATA

Supplementary Table 3. Next-generation sequencing data for FAH2 treated mice. See attached Excel file. #1 and #2 are biological replicate. Indel and snp for each sample is shown. FAH2=*Fah*$^{mut/mut}$ mice injected with FAH2, Mut=*Fah*$^{mut/mut}$ mice injected with unguided Cas9. WT=Wild-type mice.

Supplementary Table 4. Next-generation sequencing data for off-target analysis of FAH2. See attached Excel file. FAH2OT1, 3, 4 indicate off-target sites 1, 3, 4 presented in FigS5.

Methods

Construction of CRISPR vectors

pX330 vector expressing Cas9 and sgRNA[2] was digested with BbsI. Oligos for each targeting site were annealed, phosphorylated by T4 PNK, and ligated with linearized pX330 vector.

Mice and hydrodynamic injection

All animal study protocols were approved by the MIT Animal Care and Use Committee. $Fah^{mut/mut}$ mice[8] were kept on 10mg/L NTBC water. Mice with more than 20% weight loss were humanely euthanized according to MIT guidelines. Vectors for hydrodynamic tail vein injection were prepared using the EndoFreeMaxi Kit (Qiagen). 199nt ssDNA ultramer oligo was from IDT. For hydrodynamic liver injection, plasmid DNA (60 μg) and ssDNA oligo (60μg) suspended in 2ml saline were injected via the tail vein in 5-7 seconds into 8-10 weeks old $Fah^{mut/mut}$ mice. Mice were kept off NTBC water at 3 days post injection. FAH2 mice were harvested at 30 days after NTBC water withdrawal for histology, DNA and RNA analysis and FAH1/3 mice were harvested at 28 days after the second round of NTBC withdrawal. Control mice off NTBC water were harvested when reaching >20% weight loss. For measuring initial repair rate, $Fah^{mut/mut}$ mice were injected with plasmid DNA and kept on NTBC water. Livers were harvested for IHC at 6 days post injection. 8 weeks old female FVB mice from Jackson lab were injected with 60μg plasmid DNA and monitored for body weight.

Immunohistochemistry and Serum biochemistry

Mice were sacrificed by carbon dioxide asphyxiation. Livers were fixed with 4% paraformaldehyde (PFA), embedded in paraffin, sectioned at 5 μm and stained with hematoxylin and eosin (H&E) for pathology. Liver sections were de-waxed, rehydrated and stained using standard immunohistochemistry protocols[16]. The following antibodies were used: anti-Fah (Abcam, 1:400), anti-FLAG (Sigma, 1:2000). The number of positive cells was quantified from >3 regions per mouse in 3 mice per group. Blood was collected using retro-orbital puncture before each group of mice was sacrificed. ALT, AST and bilirubin levels in serum were determined using diagnostic assay kits (Teco Diagnostics).

Gene expression analysis, RT-PCR and qPCR

RNA was purified using Trizol (Invitrogen) and reverse-transcribed using a High-Capacity cDNA Reverse Transcription Kit (Applied Biosystems). Real-time PCR (qPCR) reactions were performed using gene specific primers (Applied Biosystems). Data were normalized to Actin.

Off-target analysis, surveyor assay and Illumina sequencing

Mouse 3T3 cells were stably infected with $HRas^{V12}$ to enhance transfection efficiency. 3T3 cells expressing HRas were then transiently transfected with pX330.Fah sgRNA1-3 using FugeneHD. Fah genomic region was PCR amplified. Off-target sites were predicted using http://crispr.mit.edu/[2]. For surveyor assay, PCR products were gel purified, treated with Suveryor nuclease kit (Transgenomic), and separated on ethidium bromide stained 4-20% Novex TBE Gels (Life Technologies).

Fah on-target and/or off-target PCR products were column purified or gel-purified (Zymo). Deep sequencing libraries were made from 1~100 ng of the PCR products using Nextera protocol (Illumina). Libraries were normalized to approximately equal molar ratio, and sequenced on Illumina MiSeq machines (150bp, paired-end). Reads were mapped to the PCR amplicons as references using bwa with custom scripts. Data processing was performed according to standard Illumina sequencing analysis procedures.

Statistics P values were determined by Fisher's exact test, Student's t-tests and One-Way ANOVA using Prism 5 (GraphPad).

Supplementary Discussion

Recent studies showed that long-term Cas9/sgRNA expression is not toxic in cells[17-19]. To investigate the safety of CRISPR in mice, we injected a cohort of wildtype FVB mice with unguided Cas9 plasmid or a Cas9 plus a sgRNA targeting GFP via hydrodynamic injection. Three months later, the Cas9 or Cas9/sgRNA mice were indistinguishable with respect to body weight compared to saline controls (Supplementary Fig.7a). Histopathological analysis revealed neither obvious pathological changes in the liver nor any signs of hyperplasia (Supplementary Fig.7b). These data indicate that transient expression of CRISPR/Cas9 in the liver is well-tolerated in mice. Whether longer term expression of Cas9 is well-tolerated in the liver is an important avenue of future investigation.

To examine the rate of potential CRISPR plasmid DNA integration and expression in the liver, we injected pX330 plasmids into a cohort of wildtype FVB mice and measured the expression of FLAG tagged Cas9 by IHC staining using a FLAG tag antibody. As shown in Supplementary Fig.8, an average of 16.76% FLAG positive hepatocytes at one day post injection was detected. In contrast, FLAG IHC staining was detected in 0.26±0.06% and 0.06±0.11% of hepatocytes after 1 month and 3 months post injection, respectively. These data suggest that integration of vector DNA is minimal in the liver.

To our knowledge, hydrodynamic DNA delivery has been tested in only one human clinical trial[20] and associated with hepatotoxicity[10] and the potential plasmid integration. Despite these issues, it is interesting to reconsider the potential application of hydrodynamic delivery for diseases where a single treatment would result in genetic correction of disease. We observed that FAH2 also introduced indels at the predicted Cas9 cutting site, which is consistent with the literature that Cas9 induced DSBs are repaired by both NHEJ and HDR when ssDNA is provided[1]. In the $Fah^{mut/mut}$ mice, such NHEJ events are unlikely causing phenotype because unrepaired Fah mRNA is not stable[8].

Nature Biotechnology: doi:10.1038/nbt.2884

Supplementary Reference:

16. Xue, W. et al. Response and Resistance to NF-kappaB Inhibitors in Mouse Models of Lung Adenocarcinoma. *Cancer Discov.* **1**, 236-247 (2011).
17. Shalem, O. et al. Genome-Scale CRISPR-Cas9 Knockout Screening in Human Cells. *Science* (2013).
18. Wang, T., Wei, J.J., Sabatini, D.M. & Lander, E.S. Genetic Screens in Human Cells Using the CRISPR/Cas9 System. *Science* (2013).
19. Malina, A. et al. Repurposing CRISPR/Cas9 for in situ functional assays. *Genes Dev* **27**, 2602-2614 (2013).
20. Khorsandi, S.E. et al. Minimally invasive and selective hydrodynamic gene therapy of liver segments in the pig and human. *Cancer Gene Ther* **15**, 225-230 (2008).

Nature Biotechnology: doi:10.1038/nbt.2884